New insights in the role of turbulence for simulating primary breakup of prefilming airblast atomization

K. Warncke*, A. Sadiki, J. Janicka
Department of Eergy and Power Plant Technology,
Technische Universität Darmstadt, Germany
*Corresponding author: warncke@ekt.tu-darmstadt.de

Abstract
Details of the liquid fuel disintegration in aircraft engines are not completely understood. Complex flows, a dense spray and fine liquid droplets demand high resolution and limit experimental and numerical studies. Getting access to the physical mechanisms and spray characteristics of the initial atomization step, the embedded DNS methodology has been proven to be a valuable tool: A Direct Numerical Simulation (DNS) of the primary breakup is embedded in a Large Eddy Simulation (LES) of the atomizer, reducing computational costs and making expensive DNS feasible for technical relevant applications. A specific feature of the method is the consideration of a realistic turbulent nozzle flow instead of setting constant values at the boundaries of the DNS. In this study the relevance of the inclusion of the turbulent nozzle flow in primary breakup simulations of airblast atomization is demonstrated. Therefore, a sensitivity study for a planar prefilming airblast atomizer is conducted applying one operating point and two different sets of boundary data for the embedded domain. The first set consists of time-varying data from LES of the planar atomizer while the second one considers time-averaged values of the first set. The last mentioned set mimics a constant profile at the boundaries. 3D DNS of both cases is performed applying the Volume of Fluid method. Analyses of the liquid film development and spray characteristics relating to the different amounts of turbulent scales in the gaseous flow are presented. The results indicate a non-neglectable influence of turbulence on the breakup. In particular, the results show that turbulent scales in the gaseous flow increase the amount of fine droplets. The SMD is reduced from 182 µm to 148 µm and the atomized mass is increased by 10 % if a turbulent flow is considered. Therefore, the effects of turbulence should be considered.

Keywords
Aircraft engine, fuel atomization, droplet distribution, embedded DNS, Volume of Fluid, turbulent boundary conditions.

Introduction

In aircraft engines prefilming airblast atomizers are utilized to atomize the liquid fuel. Due to high Reynolds and Weber numbers, the two-phase flow is complex and details of the dense spray in the immediate vicinity of the nozzle outlet are not accessible. Especially, droplet distributions of the initial atomization step (primary breakup) are a missing link for a detailed prediction of the combustion with Euler-Lagrange Simulations. Here, the initial droplet size distribution needs to be prescribed.
Experimental studies of generic configurations exist, analyzing influences of varying gas or liquid velocities, different liquid properties or geometrical parameters [1-4]. A first model for primary breakup of prefilming airblast atomizers were developed by Chaussonnet et al. [3]. However, for the wide range of operating conditions during a flight, suitable models are not available.
Direct numerical simulations could help to access the details of primary atomization. However, due to a required resolution in the range of micrometers in order to resolve the atomized droplets, they are limited to small domains. A DNS of an entire airblast nozzle geometry is not feasible. Here, the embedded DNS (eDNS) concept closes a gap: The DNS domain is reduced to the primary breakup region and embedded in a LES of the atomizer. Therefore, the costly DNS is reduced to the relevant region, non-neglecting the realistic turbulent nozzle flow. Several studies have proven the applicability of the eDNS for prefilming atomizers [5-7]. One important aspect of eDNS is the inclusion of a turbulent gaseous flow in primary breakup simulations. A contrary approach for the boundaries of the DNS domain would be the utilization of constant velocity profiles neglecting any impact of turbulence. A first impression of a changed liquid film breakup related to a turbulent flow is given in [5]. Though, details of the role of turbulence for prefilming airblast atomization are not known.
This study is a first step to characterize the influence of turbulent scales on the primary breakup. For this purpose, a single operating point for a planar prefilming atomizer is investigated utilizing first the eDNS method and second

a constant gas flow at the boundaries of the DNS. A systematic analysis of the temporal liquid film evolution and spray characteristics is done.
The paper is organized as follows: first the numerical eDNS concept is introduced followed by the numerical methods for LES and DNS. Afterwards, the numerical setup is explained, including a validation of the LES data applied to the embedded Domain. Subsequently, the post-processing routines for extraction of droplet statistics are summarized. Concluding, results are presented, particularly the global liquid film evolution, snapshots of single breakup events and droplet distributions in order to discuss the turbulence impact.

Numerical method

The numerical concept utilized in this study is the embedded DNS (eDNS) methodology. Sauer et al. introduced the method for simulating aircraft related airblast atomization [6]. eDNS is a tool for facilitating detailed numerical simulations of technical relevant applications by reducing the DNS to a specific region of interest, that is embedded in a LES of the investigated application. Simulating the primary atomization of prefilming airblast nozzles the DNS domain is reduced to the primary breakup zone in the vicinity of the atomizing edge of the prefilmer (Figure 1 (a)). A LES of the gaseous nozzle flow provides a realistic turbulent flow field for the DNS domain. By this procedure the liquid fuel disintegration is simulated including the realistic turbulent nozzle flow. In this study a simplification of the annular atomizer to a planar design inspired by Gepperth et al. [4] is investigated. The planar prefilmer is wetted with liquid fuel and passed by an upper and a lower air flow. Analogously to the annular design the embedded domain is placed at the prefilmer trailing edge as illustrated in Figure 1 (b). Extensive studies of the generic atomizer type proved the applicability of the eDNS concept [5-7] . A comparative study with experimental data in [5] showed a good prediction of the liquid fuel breakup and droplet size distribution.

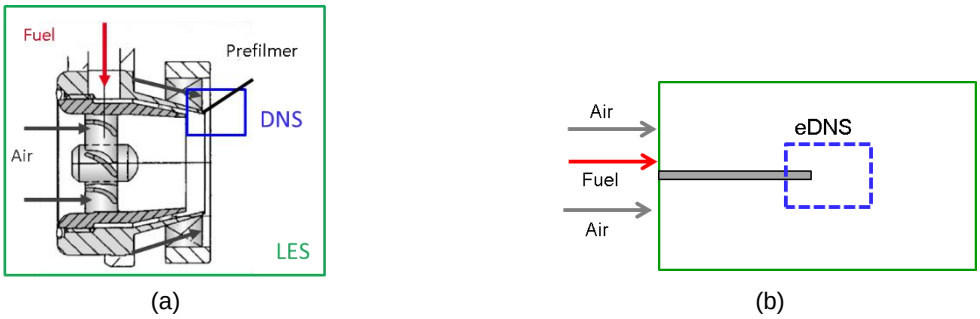

Figure 1. Embedded DNS concept for (a) annular and (b) generic atomizer design.

For the gaseous flow of the planar atomizer a single-phase LES, utilizing the pimpleFoam solver of the open source C++ library OpenFOAM, is performed. With LES the large scales are resolved whereas the small unresolved scales need to be modeled. This separation is obtained by filtering of the Navier-Stokes equations. For a Newtonian constant density flow the relevant equations are the filtered continuity equation (1) and the filtered momentum equation (2), formulated with the velocity vector of the resolved scales $\bar{\boldsymbol{U}}$, the modified kinematic pressure $\bar{P}$, the kinematic viscosity ν and the subgrid-scale viscosity ν_{sgs} of the residual content. Closure of equation (2) is obtained by modeling the subgrid-scale viscosity. In this study the Wall-Adapting Local Eddy-Viscosity (WALE) model by Nicoud and Ducros [8] is applied.

$$\boldsymbol{\nabla} \cdot \bar{\boldsymbol{U}} = 0 \tag{1}$$

$$\frac{\partial \bar{\boldsymbol{U}}}{\partial t} + \boldsymbol{\nabla} \cdot (\bar{\boldsymbol{U}}\bar{\boldsymbol{U}}) = -\boldsymbol{\nabla}\bar{P} + \boldsymbol{\nabla} \cdot \left((\nu + \nu_{sgs})(\boldsymbol{\nabla}\bar{\boldsymbol{U}} + (\boldsymbol{\nabla}\bar{\boldsymbol{U}})^T) \right) \tag{2}$$

To simulate the primary atomization in the eDNS domain the multiphase solver InterFoam of OpenFOAM is used. In InterFoam the Volume-of-Fluid (VOF) method is implemented to capture the liquid-gas interface. Central element of VOF is an indicator function α that represents the volume ratio of liquid to gas inside a computational cell. The physical properties, as density and viscosity, are calculated as a function of the indicator following equations (3) and (4).

$$\rho = \alpha\rho_l + (1-\alpha)\rho_g \tag{3}$$

$$\mu = \alpha\mu_l + (1-\alpha)\mu_g \tag{4}$$

The momentum equation (6) under the incompressibility constraint (5) is modified in order to account for effects of surface tension ruled by the interface curvature κ, calculated with equation (7). The surface tension force cannot

be determined directly, therefore, a volume force, that is effective in the transition region, is formulated instead. This method is known as the Continuum Surface Force (CSF) method by Brackbill et. al [9]. The transport of the phase interface is described by an additional advection equation (8) utilizing the indicator. The interface is smeared in a region from 0 to 1.The last term on the left side is only active in the proximity of the phase interface and represents an artificial compression term antagonizing numerical diffusion [10]. No geometrical reconstruction of the phase interface is applied.

$$\boldsymbol{\nabla} \cdot \boldsymbol{U} = 0 \tag{5}$$

$$\frac{\partial \rho \boldsymbol{U}}{\partial t} + \boldsymbol{\nabla} \cdot (\rho \boldsymbol{U}\boldsymbol{U}) = \rho \boldsymbol{g} - \boldsymbol{\nabla} p + \boldsymbol{\nabla} \cdot [\mu(\boldsymbol{\nabla}\boldsymbol{U} + (\boldsymbol{\nabla}\boldsymbol{U})^T)] + \sigma \kappa \boldsymbol{\nabla} \alpha \tag{6}$$

$$\kappa = -\boldsymbol{\nabla} \cdot \left(\frac{\boldsymbol{\nabla}\alpha}{|\boldsymbol{\nabla}\alpha|} \right) \tag{7}$$

$$\frac{\partial \alpha}{\partial t} + \boldsymbol{\nabla} \cdot (\alpha \boldsymbol{U}) + \boldsymbol{\nabla} \cdot \left(\boldsymbol{U}_r \alpha (1-\alpha) \right) = 0 \tag{8}$$

Numerical set-up

The generic atomizer simulated in this study is illustrated in Figure 2. A planar prefilmer is placed inside a channel, subdividing the front part into two separate channels with height $H = 2\delta$ and length $L_{z,1} = 2\pi\delta$. The channel half height δ corresponds to the experimental set-up in [5] and measures 4 mm. The turbulent channel flows above and below the prefilmer are recycled and operate as turbulent inflow generators for the adjacent atomization unit with length $L_{z,2} = 3\pi\delta$. The prefilmer length in the last unit is $\pi\delta$. The spanwise x-direction measures $L_x = \pi\delta$ and periodic boundary conditions are set. The grey faces are treated as walls with a no-slip condition. The gaseous flow leaves the domain at the outlet on the right hand side. The position of the eDNS domain is highlighted in the vicinity of the prefilmer trailing edge. It should be noted that the two-phase DNS is performed separately. At the blue planes inside the LES domain the velocity field at each LES time step is extracted and stored. The extracted data is mapped to the corresponding boundaries of the DNS domain. As time step and grid size of the LES are coarser than in the DNS, a linear interpolation in time and space is applied to map the data. The data are defined as transient Dirichlet boundary condition for each individual time step. The turbulent fluctuations are directly transferred to the DNS domain. The liquid fuel enters the DNS domain through a small liquid slit above the prefilmer.

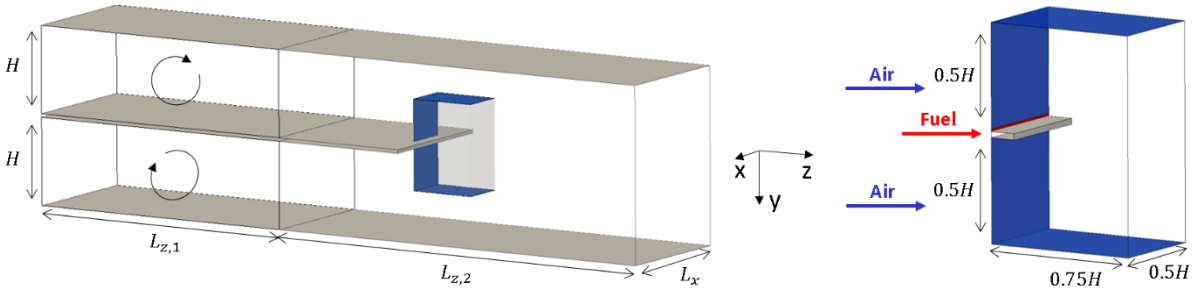

Figure 2. Computational domain of planar atomizer design. Left: LES domain and position of embedded domain. Right: DNS domain.

The conditions of the investigated operating point are identical chosen to [5] and summarized in Table 1. The bulk velocity of the turbulent channel flow is set to 50 m/s at ambient conditions. The liquid properties correspond to Shellsol D70, a fuel surrogate with properties close to aviation fuels, as utilized in [4, 5].

Table 1. Operating conditions.

Parameter	Unit	Value
u_{gas}	m/s	50
ρ_{gas}	kg/m³	1.2
ν_{gas}	m²/s	1.53e-05
u_{liquid}	m/s	0.5
ρ_{liquid}	kg/m³	770
ν_{liquid}	m²/s	2.03e-6
σ	kg/s²	0.0275

LES of generic atomizer

The numerical grid of the LES of the generic atomizer comprises 21.24 m cells. Equidistant grid spacing in streamwise z- and spanwise x-direction are applied. In wall-normal y-direction the grid size is stretched from the wall to the core of the channels. Near wall resolution is achieved. The non-dimensional grid sizes in x-/y-/z-direction are 10.9/1.8-45.8/21.8. The sampling of the velocity data for the DNS domain is started once a statistically stationary state of the flow is reached.

The results of the LES are validated against DNS data of Iwamoto [11] (Figure 3). First and second order statistical moments of velocity at the channel half length $L_{z,1}/2$ are compared to the turbulent channel flow DNS. The rms velocity profiles include besides the filtered also the residual contribution given by the residual stress tensor. For its calculation the turbulent kinetic energy of the subgrid scales is modeled with an algebraic approach of Lilly [12]. The mean velocity profile is in excellent agreement with DNS data. For the rms velocity profiles a good agreement with minor differences to the reference data is observed. The peak value of the axial component as well as the log-law region of the x- and y-components are slightly overestimated. At the buffer layer, the x- and y-components are underestimated. Overall, the physics of the turbulent flow are reproduced in good quality by the LES assuring a reasonable flow field for the two-phase DNS.

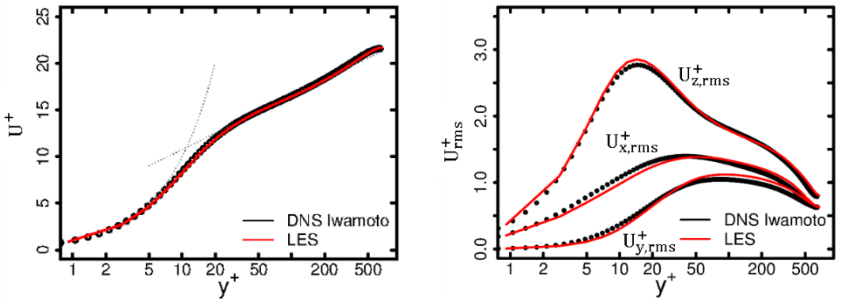

Figure 3. (a) Mean velocity profile and (b) rms velocity profile of the turbulent channel flow (Re_τ=694) prior to the atomizer unit compared to the DNS data of Iwamoto at Re_τ=643.

Two-phase DNS of primary breakup

The embedded DNS domain comprises the prefilmer lip and the atomization region as illustrated in Figure 4. An air flow inlet is sited each above and below the prefilmer. The liquid fuel enters the domain through a small slit ($h_{film,} = 0.1\ mm$), is transported along the prefilmer and exposed to high shear forces induced by the coflowing air streams. The liquid accumulates at the prefilmer trailing edge and is atomized downstream of the trailing edge. The prefilmer thickness is $h_{edge} = 230\ \mu m$. The domain measures 4.00 x 8.33 x 6.00 mm in x-, y- and z-direction. The prefilmer length is 1 mm.

The liquid fuels enters the domain with a constant velocity. The faces of the prefilmer are treated as walls with a no-slip condition and outlet conditions are assigned to the outlet of the domain. A slip condition is assigned to the lateral faces, the normal component is set to zero and the tangential components are initialized as zero gradients. The coflowing air next to the prefilmer is directly linked to the gaseous flow in the LES. The sampled velocity data during the LES is mapped onto the *InletTop*, *InletBottom*, *Top* and *Bottom* faces as transient Dirichlet boundary conditions. An example for the mapped velocity field is shown in Figure 4.

The extension of the numerical domain in y-direction is chosen in a way, that the predefined flow field at the top and bottom boundaries do not influence liquid film breakup. As primary atomization is located in the vicinity of the trailing edge, the numerical grid is divided in a core zone 4.00 x 4.33 x 6.00 mm with equidistant grid spacing of 10 µm in all three directions and two outer zones with doubled grid size above and below the core zone. The total number of cells is 115 million. An estimation of the Kolgomorov scales can be found in [6]. The ratio of the grid size to the Kolgomorov scales Δ/η satisfies the criterion $\Delta/\eta < 2.1$ of Pope [13] in the complete numerical domain to resolve the smallest turbulent scales.

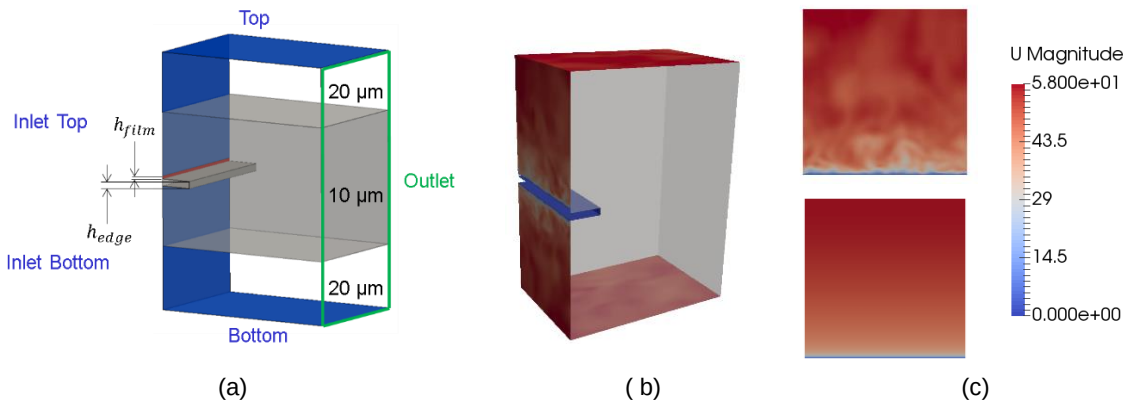

Figure 4. (a) Embedded DNS domain divided in core and outer zones, (b) mapping of the LES velocity data and (c) the velocity field at InletTop for the cases ULes (top) and UMean (bottom).

To analyze the influence of turbulent scales on the primary breakup two cases are distinguished in this study. First, the turbulent flow resolved by the LES is utilized for the simulation of primary breakup of the liquid film (denoted as case ULes in the following). Secondly, the extracted LES data is time-averaged and the corresponding constant velocity profile, as shown in Figure 4 (c) for *InletTop*, is imposed at the four coupling planes. The bulk velocity is identical in both cases. A physical time period of 16 ms is calculated in either case.

Post-Processing and droplet analysis

The implemented post-processing routine for detection of all liquid structures produced by primary atomization is based on a Connected Component Labeling (CCL) algorithm applied to the 3D DNS domain. Based on a predefined α-threshold the content of each grid cell is identified as liquid or gas and labelled accordingly with 1 or 0 (Figure 5). The threshold is set to $\alpha = 0.5$. The CCL algorithm finds all neighbored cells containing liquid and belonging to the same liquid structure. A unique number per identified structure is assigned to the corresponding computational cells. The total volume of a single droplet is then calculated as the sum of the liquid amount in each cell i corresponding to the analyzed droplet, as formulated in equation (9). The droplet diameter is derived as equivalent diameter.

$$V_d = \sum_i \alpha_i \Delta x \Delta y \Delta z \tag{9}$$

By this procedure size and position of all droplets is recognized. A separation in the intact liquid core and droplets is possible. The droplet shape is not relevant for the detection algorithm, large and strongly deformed structures are also included just as small almost spherical droplets. The analysis window may include the complete computational domain or is reduced to a specific region of interest by choice. The time step between two consecutive snapshots of the numerical field is set large enough to avoid multiple counts of each droplet.

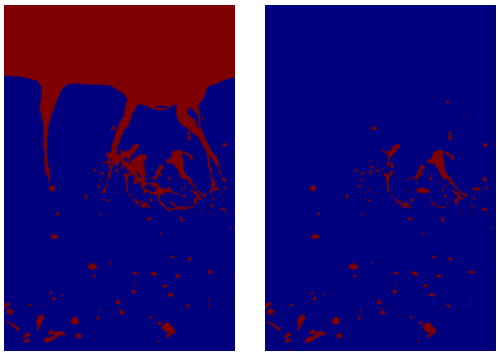

Figure 5. Left: Identification of all liquid structures and labelling with 1 (liquid, red) or 0 (gas, blue). Right: The intact liquid core is not considered in the droplet analysis.

Results and discussion

Liquid film evolution

During the primary breakup simulations two quantities related to the liquid mass were recorded over time: The total liquid mass inside the computational domain as well as liquid mass flow at the outlet. With the help of both, shown in Figure 6 for case ULes and UMean, the global liquid film evolution is analyzed.

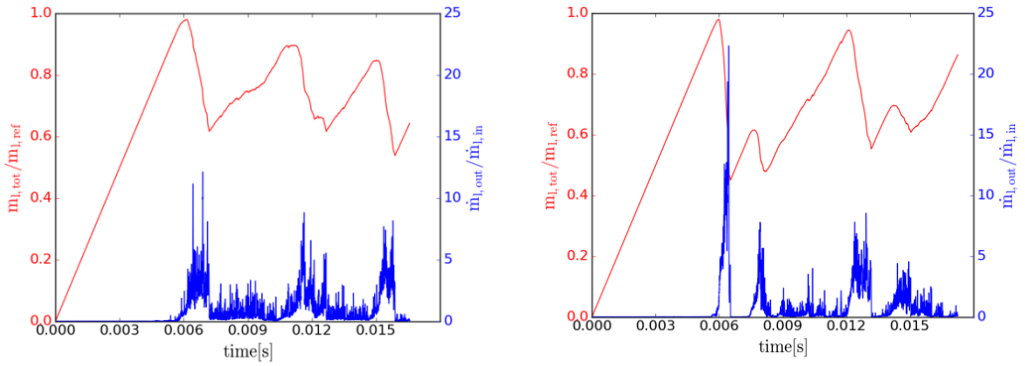

(a) (b)

Figure 6. Normalized profiles of total liquid mass in numerical domain (red) and liquid mass flow at the outlet (blue) for (a) case ULes and (b) case UMean.

As the fuel starts to enter the domain, the amount of liquid in the numerical domain is growing until a peak value is reached at 6 ms. The total liquid mass falls promptly and at the same time a peak of the liquid mass flow at the

outlet is observed. This indicates that a breakup event happened and droplets left the domain. Afterwards the process restarts and it should be noted, that no constant profiles arise. The reason is that a liquid reservoir at the prefilmer trailing edge fills before atomization takes place. The effect is seen in both simulation cases and is typical for this atomizer type [4]. The maximum accumulated liquid mass is identical in both cases and is reached immediately prior to the first breakup event. This value $m_{l,ref}$ is used to normalize the total liquid mass in Figure 6. It is apparent that different temporal profile evolutions exist, depending on which boundary conditions are applied. For turbulent (ULes) conditions three uniform peaks (main breakup events) at 6 ms, 11 ms and 15 ms are noticed, hypothesizing a characteristic breakup frequency. In the case of time-averaged (UMean) conditions all main peaks are followed by lower peaks, which increase the total breakup frequency significantly. A time series of the main breakup events is shown in Figure 7 for case ULes and case UMean.

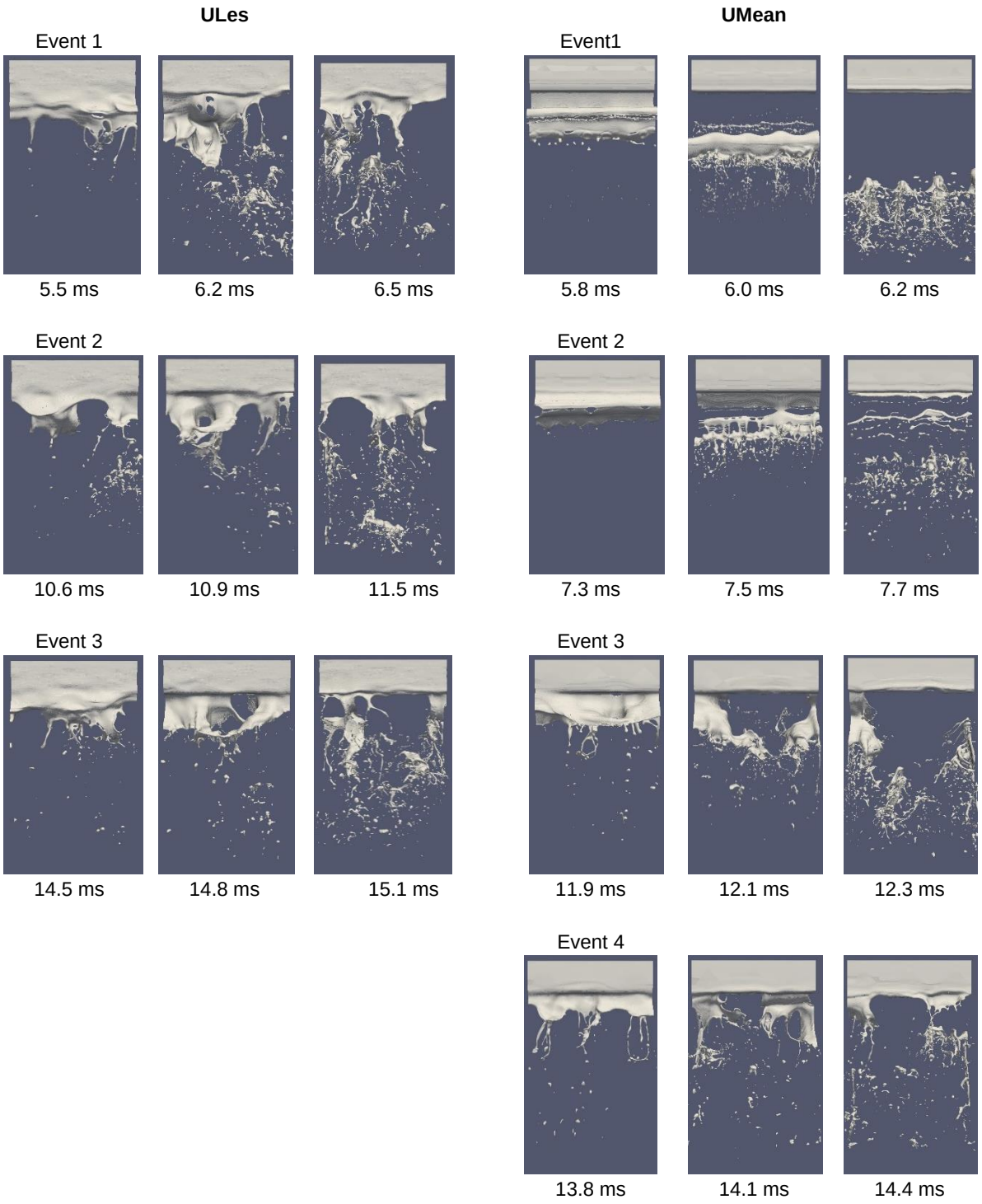

Figure 7. Liquid film evolution. Left: Influenced by turbulent velocity field from LES. Right: Time-averaged velocity profile at inlet boundaries.

When utilizing the time varying velocity field of the LES at the DNS boundaries, an irregular atomization along the prefilmer trailing edge is observed. The observed formation of bags out of the accumulated liquid is characteristic for this type of atomizer, as found in previous studies [2, 4, 5]. The bag is growing and finally bursts into fine droplets. The rim of the bag is more stable and separates first into ligaments, which are disintegrating on the way further downstream. It should be noted that no continuous liquid sheet, flapping with a constant frequency behind the trailing edge, is formed. From the first to the third breakup events all are related to the same physical mechanisms. They occur with high similarity as shown in the left column of Figure 7.
In contrast to this, the liquid film starts to develop uniformly when using a constant velocity field (UMean) at the DNS boundaries (right column of Figure 7). A continuous liquid sheet is formed behind the trailing edge, separating on the whole in the vicinity of the trailing edge (Event 1). The separated sheet disintegrates further downstream into big bulgy droplets. At Event 2 spanwise ligaments are formed from the continuous liquid film that splits parallel to the trailing edge into smaller ligaments and eventually into droplets. Again, the liquid film disintegration is uniformly along the atomizing edge. A first bag is formed not until Event 3. The bag breakup is followed by irregular disintegrations at Event 4 that show similarity to the irregular disintegration of the ULes case. Therefore it is proven that utilizing a constant velocity profile for the gaseous flow requires the liquid film to breakup several times first until a reliable result can be obtained. Contrary, the use of turbulent boundary conditions makes the prediction of characteristic breakup mechanisms viable even from the beginning of the simulation. At the end of the simulation, the mass profiles of UMean (Figure 6) still do not match the ULes profiles. It is uncertain if they will do so after a reasonable timespan.

Droplet statistics

The most interesting question is how the explicit prescribed turbulent scales affect the spray characteristics. With the help of the described post-processing routine the size of the generated droplets were extracted at the plane $z = 5\ mm$. In the procedure the first breakup event was neglected in each of the two simulation cases. The droplet size distributions for ULes an UMean are shown in Figure 8 (a). Both droplet spectra show a continuous distribution up to a diameter of $d = 250\ \mu m$. In addition, single peaks with high mass fractions are noticed for $d > 250\ \mu m$. The Sauter Mean Diameter (SMD) is higher in the case of UMean and measures 182 µm. If turbulent scales are considered (ULes) the SMD is reduced to 148 µm. Indeed, the amount of fine droplets is higher for ULes as shown in Figure 8 (b). Note that liquid structures with $d > 250\ \mu m$ are removed in Figure 8 (b). They represent ligaments and larger strongly deformed structures originating from the rim of bag breakups. The structures will breakup into droplets by secondary breakup mechanisms downstream of the outlet. Here, the discussion focuses on the fine droplets resulting from primary breakup. For these fine atomized droplets a significant increase of the mass fraction is visible in the case of ULes. The cumulative mass distribution in Figure 8 (c) verifies that for ULes 10 % more of the liquid mass are atomized to fine droplets by primary breakup. The turbulent scales induce a more intense breakup. On the other hand, it is obvious from the cumulative distribution that about half of the liquid mass is not efficiently atomized by primary breakup for the simulated configuration (53 % for UMean or 43 % for ULes). This aspect needs to be considered in Euler-Lagrange simulations once coupled with droplet data from DNS.

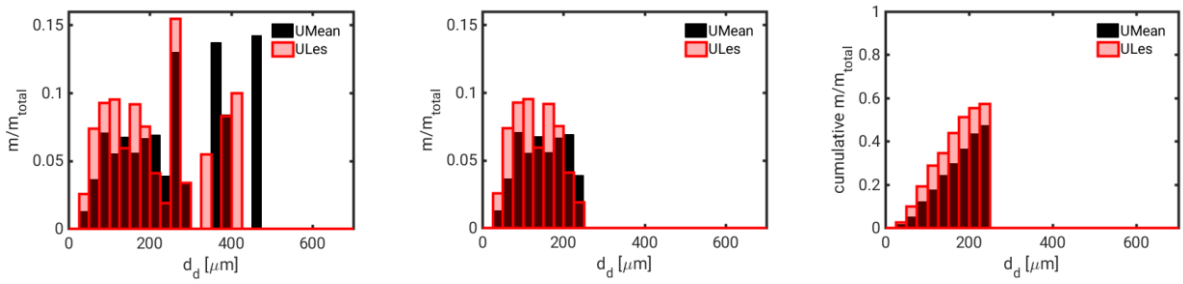

Figure 8. Droplet size distribution for the cases ULes and UMean: (a) all liquid structures, (b) primary breakup droplets with diameters $d < 250\ \mu m$, (c) cumulative mass distribution for $d < 250\ \mu m$.

Conclusions

The embedded DNS method is a useful method for the inclusion of realistic turbulent scales in the gaseous flow of primary breakup simulations of airblast atomization. Herein, turbulent velocity data of LES are mapped to DNS boundaries. In order to investigate the influence of turbulent scales on primary breakup, the present study predefines constant values at the boundaries in a second simulation case. As a result, the breakup mechanism is properly predicted from the beginning if turbulent boundary conditions are applied. For a time-averaged velocity field, several breakup events occur until the establishment of stochastic breakup behaviour is observed. Therefore, using turbulent boundary data along with the embedded DNS method is a practical means in order to

cut down cost of time consuming DNS. If time-averaged data shall be used, reasonable simulation time constraints have to be considered at the beginning.
However, even if the qualitative breakup behavior is well predicted, deviations in the temporal film evolution and breakup frequency exist. Also effects of turbulent scales on spray characteristics would be neglected. The results show that turbulent scales in the gaseous flow increase the amount of fine droplets. The SMD is reduced from 182 µm to 148 µm and the atomized mass is increased by 10 % if a turbulent flow is considered. Therefore, the effects of turbulence should be considered. The inclusion will be of practical importance, if real aircraft nozzles with a typical high turbulent intensity are simulated.

Acknowledgements
The authors would like to thank the German Research Foundation (DFG) for the financial support under contract no. JA544/39-1. Calculations for this research were conducted on the Lichtenberg high performance computer of the TU Darmstadt

Nomenclature

Abbrevations

SMD	Sauter Mean Diameter
VOF	Volume-of-Fluid

Latin Symbols

U	Velocity [m s^{-1}]
P	Modified kinematic pressure [m s^{-2}]
H	Height [m]
L	Length [m]

Greek Symbols

ν	Kinematic viscosity [m^{-2} s^{-1}]
μ	Dynamic viscosity [kg m^{-1} s^{-1}]
σ	Surface tension [kg s^{-2}]
κ	Curvature [m^{-1}]
α	Indicator function [-]
δ	Channel halh height [m]
η	Kolgomorov length scales [m]
Δ	Grid size [m]

Subscripts

sgs	Subgrid-scales
ref	Reference
l	Liquid
$film$	Liquid film
$edge$	Prefilmer trailing edge
d	Droplet
in	Inlet
out	Outlet
tot	total

References

[1] Okabe, T., Katagata, N., Sakaki, T., Inamura, T., and Fumoto, K., "Effect of Prefilmer Edge Thickness on Breakup Phenomena of Liquid Film in Prefilming Airblast Atomizer," Proc. 28th Conference on Liquid Atomization and Spray Systems.
[2] Déjean, B., Berthoumieu, P., and Gajan, P., 2016, "Experimental study on the influence of liquid and air boundary conditions on a planar air-blasted liquid sheet, Part II: prefilming zone," International Journal of Multiphase Flow, 79, pp. 214-224.
[3] Inamura, T., Shirota, M., Tsushima, M., and Kato, M., "Spray Characteristics of prefilming Type of Airblast Atomizer," Proc. 12th Triennial International Conference on Liquid Atomization and Spray Systems.
[4] Gepperth, S., Müller, A., Koch, R., and Bauer, H.-J., "Ligament and Droplet Characteristics in prefilming Airblast Atomization," Proc. 12th Triennial International Conference on Liquid Atomization and Spray Systems.
[5] Warncke, K., Gepperth, S., Sauer, B., Sadiki, A., Janicka, J., Koch, R., and Bauer, H.-J., 2017, "Experimental and numerical investigation of primary breakup of an airblasted liquid sheet," International Journal of Multiphase Flow, 91C, pp. 208-224.
[6] Sauer, B., Sadiki, A., and Janicka, J., 2016, "Embedded dns concept for simulating the primary breakup of an airblast atomizer," Atomization and Sprays, 26(3), pp. 187-215.
[7] Sauer, B., Sadiki, A., and Janicka, J., "Embedded DNS of the primary breakup of a prefilming airblast atomizer at aircraft engine operating conditions," Proc. 25th European Conference on Liquid Atomization and Spray Systems.
[8] Nicoud, F., and Ducros, F., 1999, "Subgrid-scale stress modelling based on the square of the velocity gradient tensor," Flow Turbulence Combust, 62(3), pp. 183-200.
[9] Brackbill, J., Kothe, D., and Ca, Z., 1992, A Continuum Method for Modeling Surface Tension.
[10] Rusche, H., 2002, "Computational Fluid Dynamics of Dispersed Two-Phase Flows at High Phase Fractions,"Ph.D. thesis, University of London.
[11] Iwamoto, K., 2002, "Database of Fully Developed Turbulent Channel Flow," University of Tokyo, Department of Mechanical Engineering, Tokyo.
[12] Lilly, D. K., "The representation of small-scale turbulence in numerical simulation experiments," Proc. IBM Scientific Computing Symposium on Enviromental Sciences, pp. 195-210.
[13] Pope, S. B., 2000, Turbulent Flows, Cambridge University Press, Cambridge.